Synthesis of ultrashort laser pulses for high-order harmonic generation

E. Neyra,[1] F. Videla,[1] M. F. Ciappina,[2] J. A. Pérez-Hernández,[3] L. Roso,[3] and G. A. Torchia[1,*]

[1]*Centro de Investigaciones Ópticas, CONICET-CICBA-UNLP, Camino Centenario y 506, M.B. Gonnet (1897), Province of Buenos Aires, Argentina*

[2]*Institute of Physics of the ASCR, ELI-Beamlines project, Na Slovance 2, 182 21 Prague, Czech Republic*

[3]*Centro de Láseres Pulsados (CLPU), Parque Científico, E-37185 Villamayor, Salamanca, Spain*

(Received 30 March 2018; published 3 July 2018)

We present a technique for the synthesis of ultrashort laser pulses with approximately one cycle (FWHM) of temporal duration. These pulses are characterized by a certain degree of chirp. We show that these pulses produce both an enhancement of the high-order harmonic generation (HHG) cutoff and a noticeable increase of the yield, when interacting with an atomic system. Additionally, the asymmetric nature of the driven pulses plays an important role in the efficiency and cutoff extension of the high-order harmonics generated. Starting from the HHG spectra, we demonstrate it is possible to retrieve isolated attosecond pulses by spectral filtering. The analysis and interpretation of the different characteristics present in the HHG driven by this kind of pulse was carried out invoking classic arguments. Furthermore, a more complete description and validation of the HHG properties is performed by a quantum analysis, based on the integration of the time-dependent Schrödinger equation in full dimensionality.

DOI: 10.1103/PhysRevA.98.013403

I. INTRODUCTION

In the last few years, there has been a great advance in the generation of ultrashort laser pulses with a stable carrier envelope phase. These systems can deliver sub-two optical cycles, with energies in the submillijoule regime, in the spectral range of 0.8–2 μm [1–3]. On the other hand, the synthesis of single-cycle and subcycle pulses was also achieved [4–6]. The interest in obtaining these kinds of pulses mainly relies on the possibility of generating isolated attosecond pulses (IAPs), which allow the study of atomic and molecular electronic processes at their native temporal, attosecond, scale [7,8]. It is worth mentioning that there exist other methods to generate IAPs based on multicycle driven pulses but based on polarization gating [9,10]. The flagship for the generation of these pulses is the the well known nonlinear strong field phenomenon called high-order harmonic generation (HHG). HHG is a process that takes place when high-intensity ultrashort laser pulses interact with atomic and molecular gaseous systems. This interaction generates a burst of high-energy photons, typically in the XUV to soft-x-ray spectral range. These photons have odd frequencies of the original frequency, ω_0, of the driving laser pulse.

A typical harmonic spectrum can be separated into three regions: (i) the perturbative one, where the low-order harmonics yield decays, (ii) a plateau, where all harmonics have a similar intensity, confirming the nonlinear nature of the process, and (iii) an abrupt cutoff at a maximum photon energy that can be calculated classically [11–13].

When a high-intensity laser pulse interacts with an atom or molecule, it causes a deformation of the Coulomb potential and this enables the tunnel ionization of one or more electrons. Once in the continuum, the electrons are accelerated by the external electric field and driven back to recombine with the parent ion emitting their excess energy in the form of high-energy photons. The maximum photon energy E_{cutoff} is proportional to the U_p, the ponderomotive energy, which in turn can be written as $U_p \propto I\lambda^2$. Consequently, there are two possible routes to extend the harmonic cutoff, namely, to increase (i) the laser wavelength or (ii) the laser intensity. However, a longer wavelength will imply an abrupt decreasing of the HHG efficiency, which scales as $\lambda^{-5.5}$ [14–17]. The reasons for this reduction can be traced out in the spreading of the electron wave packet, because there is an increase of the trajectory duration $\tau \propto \lambda$ [14,17]. In addition an increment in the intensity will also entail a loss of efficiency when the saturation intensity, characteristic of the target atom, ion, or molecule, is exceeded [18–20]. Recently an avenue was demonstrated to extend the HHG cutoff driving the active media with a temporal and spatial synthesized field, although the experimental realization is still challenging [21,22].

In this paper, we present a technique for the synthesis of ultrashort pulses jointly with a theoretical analysis of its interaction with a noble gas. We focus our study on argon because it is a rare gas commonly used in HHG experiments. Our approach allows obtaining chirped ultrashort pulses with approximately one cycle of temporal duration (FWHM). By starting with an optical pulse with central wavelength λ_0 and a temporal duration range from one cycle to and one and a half cycles FWHM, we obtain optical pulses with $\lambda \approx 1.5\lambda_0$. To perform this temporal synthesis, we superimpose two pulses with different degrees of chirp. In order to achieve this goal it is not needed to employ a nonlinear medium; using a dispersive medium is enough. As we will see in the next sections, the instrumental parameter is the group velocity dispersion (GVD).

The theoretical study of the HHG driven by the synthesized pulses has been made by solving the time-dependent

*gustavot@ciop.unlp.edu.ar

 ©2018 American Physical Society

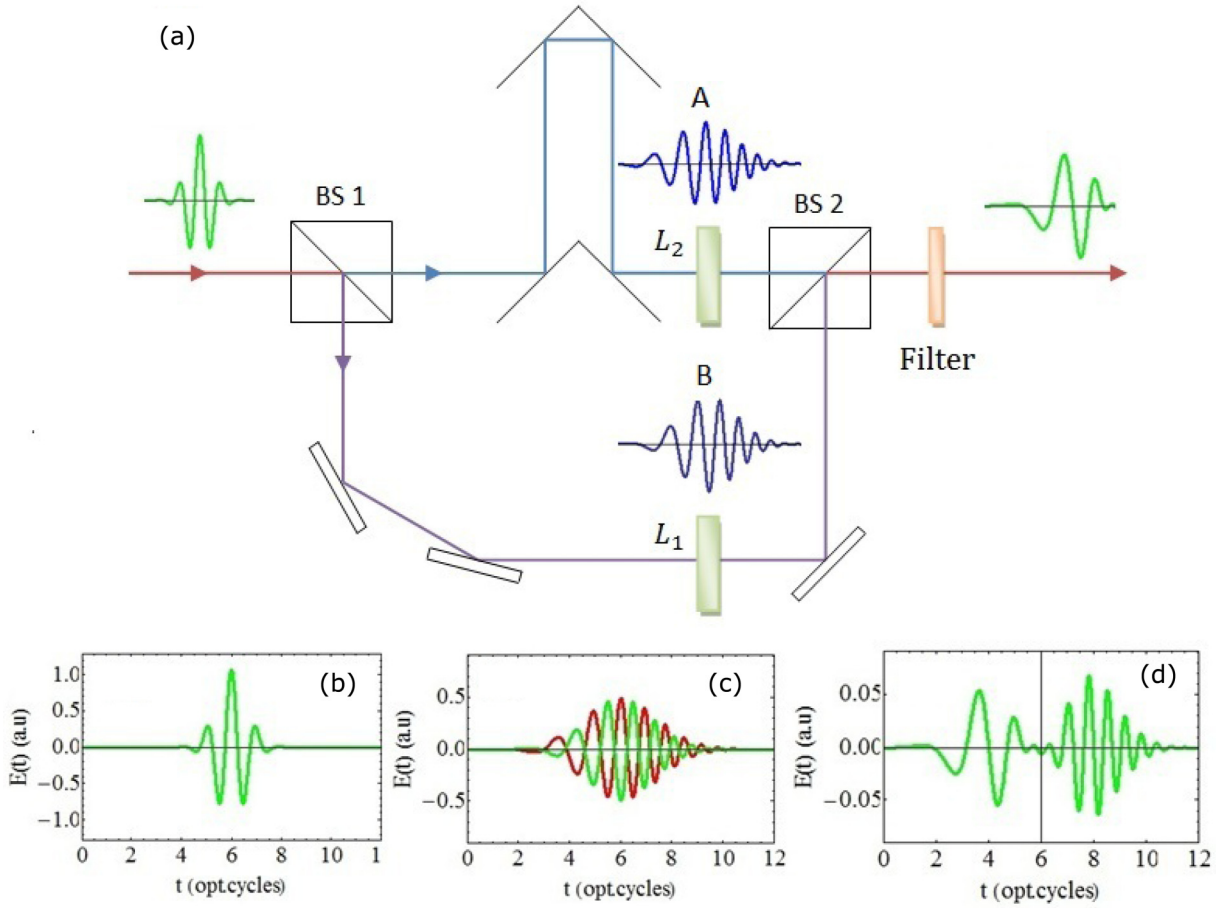

FIG. 1. Potential experimental setup to carry out the proposed pulse synthesis.

Schrödinger equation in full dimensionality (3D-TDSE) using argon as a target atom under the single active electron (SAE) approximation. Additionally the classical analysis of HHG characteristics is performed by solving the Newton-Lorentz equation.

The pulses synthesized by our technique have certain asymmetric characteristics in the pulse period. This means that the temporal region of the optical pulse when the electron is ionized is different from the one which enables its recombination. This asymmetry causes noticeable changes in the electron trajectory in comparison with a conventional sine-squared or Gaussian pulse. A clear increase of the electron recombination energy is obtained, depending on the kind of asymmetry in the pulse. This, in turn, translates to an extension of the HHG cutoff. Besides, the electron travel time in the continuum will be different and this indeed improves the efficiency of the HHG, as mentioned before. In previous contributions, some authors proposed different ways of obtaining this asymmetry in one period of the optical pulses, e.g., using the so-called perfect wave or summing up pulses with same and different colors, among others [21,23–28]. In these articles, a cutoff extension of the HHG spectrum and/or an enhancement in the harmonic yield are obtained depending on the synthesized pulse. In our approach, both of the mentioned effects in the HHG spectrum are achieved.

II. METHODS

A. Pulse synthesis

For the synthesis of the pulses we propose the experimental setup depicted in Fig. 1(a). In this scheme, we achieve the sum of two pulses with different degrees of chirp (GVD) and a π phase change between of them. In summary, we present the synthesis of four pulses varying the sign and degree of chirp of the initial pulses A and B.

Initially we have a Gaussian pulse with a central wavelength λ_0 and one cycle of FWHM [Fig. 1(b)]. This pulse is divided into two pulses, pulse A (PA) and pulse B (PB), through a beam splitter (BS). PB crosses a dispersive media with length L_1 and is reflected by a number of odd mirrors. On the other hand, PA crosses a dispersive medium with length L_2 and travels through the same optical path, but the mirrors that reflects it are an even number. This originates then a phase change in π with respect to PB. Next, the two pulses merge in a beam splitter. The representation of these pulse superpositions is showed in Fig. 1(c). Furthermore, in Fig. 1(d) we depict the temporal sum of these pulses. As can be seen, we obtain a new pulse that has two distinct spectral zones, each of them with a different wavelength. One of these regions has an approximate wavelength $\lambda \approx 1.5\lambda_0$ and a one-cycle FWHM, while the other one has a shorter wavelength, irrelevant to our study (note that

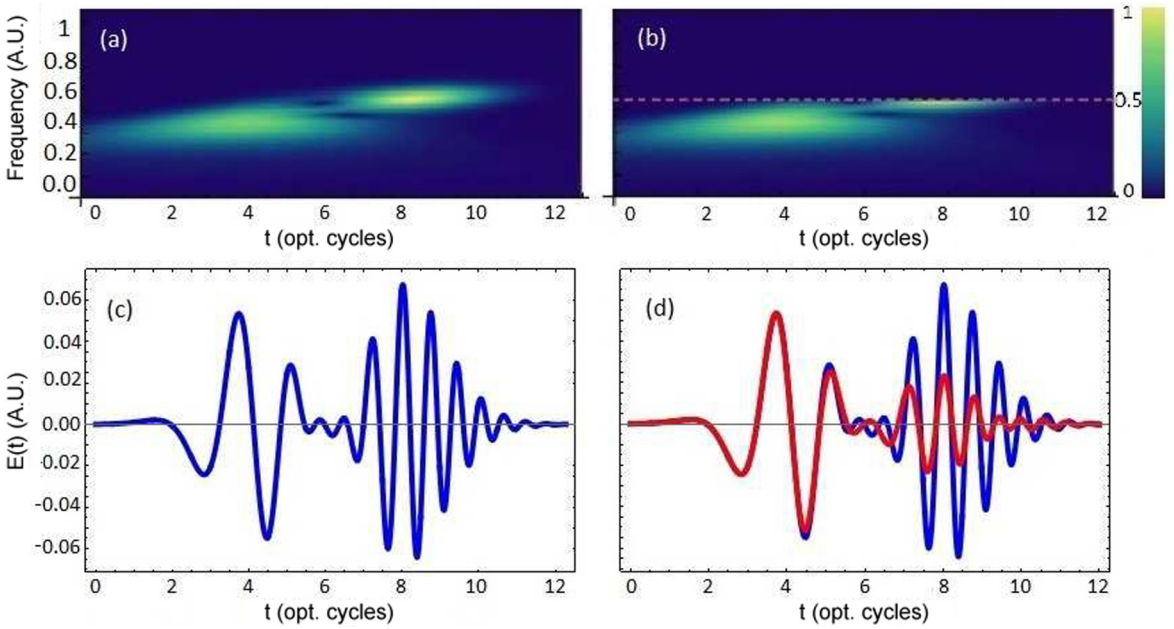

FIG. 2. Wavelet analysis of the (a) synthesized and (b) filtered pulses. Temporal profiles of the (c) synthesized and (d) filtered (in red) pulses.

it may be important for other applications). For this reason, we propose an optical filter to remove this higher frequency region [Fig. 1(a)].

Considering the broad spectral range of the two pulses, they are a few femtoseconds FWHM long, and there is clear temporal separation [Fig. 1(d)], so the wavelet analysis of the synthesized pulse is a good choice for understanding the effect of the proposed ideal optical filter. In Fig. 2(a) we show the wavelet analysis of the synthesized pulse [Fig. 2(c)]. In this case two regions are clearly observed, each temporarily centered, at four and eight optical cycles, respectively. As expected, these two regions show different spectral content. The optical filter then was applied in order to keep the total spectral composition over the pulse at low frequencies, as

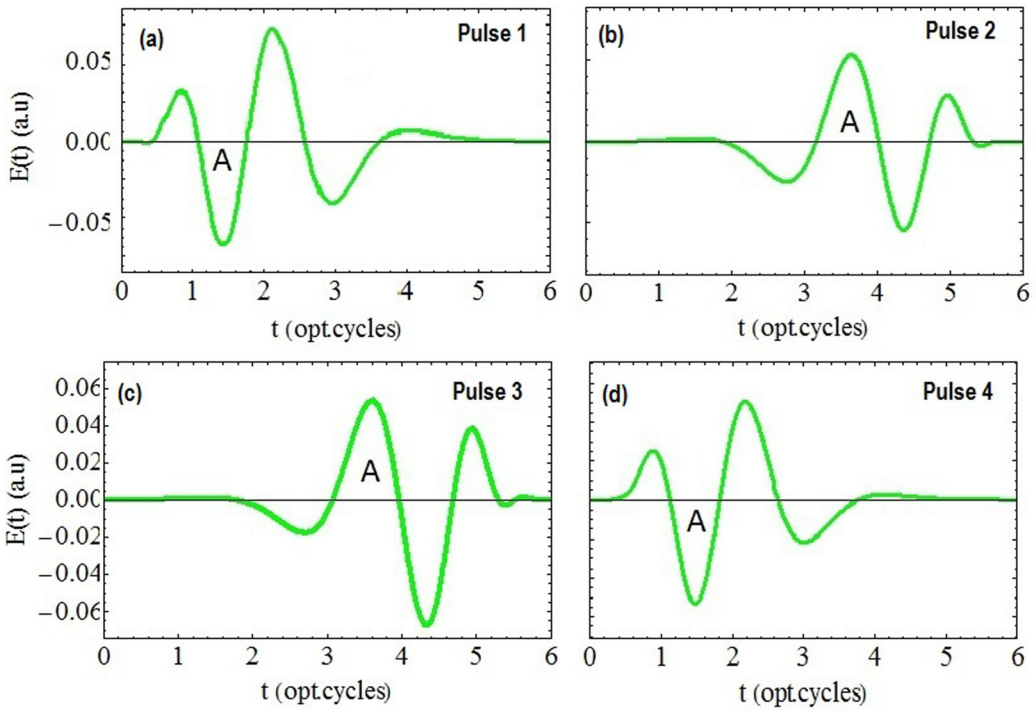

FIG. 3. Temporal profile of the four pulses synthesized in the present study. (a) Pulse 1 is obtained with $L_1 = 25\ \mu$m, $L_2 = 30\ \mu$m and it is up-chirped; (b) pulse 2 with $L_1 = 25\ \mu$m, $L_2 = 30\ \mu$m and down-chirped; (c) pulse 3 with $L_1 = 20\ \mu$m, $L_2 = 30\ \mu$m and up-chirped; (d) pulse 4 with $L_1 = 20\ \mu$m, $L_2 = 30\ \mu$m and down-chirped. Note that the temporal region corresponding to higher frequencies was removed ($t > 6$ optical cycles).

shown in Fig. 2(b). Figure 2(d) shows in the red dashed line the pulse obtained after crossing the ideal optical filter and in blue the original pulse. As observed of the figure, the filtered pulse does not change its form in the first part (which is of our interest), but in the second one its amplitude decreases dramatically. We demonstrated in a previous work that the second part of the pulse has no influence on the HHG process, since its amplitude is not enough to ionize the atom [26].

After the high-frequency region removal, the four synthesized pulses are shown in Fig. 3. Each of the pulses was obtained by varying the length L_1 and L_2 and the sign of the chirp (up-chirp or down-chirp). The dispersive medium used was an SF14 glass [26]. In order to achieve pulses 1 and 2 [Figs. 3(a) and 3(b)], the lengths of the media were $L_1 = 25\,\mu$m and $L_2 = 30\,\mu$m and pulse 1 wasw up-chirped while pulse 2 was down-chirped. Likewise, the lengths of the media to obtain pulses 3 and 4 [Fig. 3(c) and 3(d)] were $L_1 = 20\,\mu$m and $L_2 = 30\,\mu$m. Here pulses 3 and 4 were up- and down-chirped, respectively. In this representation the second part ($t > 6$ optical cycles) of the optical wave for each case was removed, since it has no important effects on the HHG.

B. Theoretical methods

According to the three-step model [11,29,30] the maximum photon energy E_{cutoff} in every harmonic spectrum is given by the semiclassical cutoff law

$$E_{\text{cutoff}} = I_p + 3.17U_p \tag{1}$$

(atomic units are used throughout this paper unless otherwise stated), where I_p is the ionization potential of the corresponding atom or ion target (in this work we focus our study on the argon atom, $I_p = 0.57$ a.u., i.e., 15.7 eV), ω_0 is the central laser frequency, and U_p is the ponderomotive energy given by

$$U_p = \frac{E_0^2}{4\omega_0^2}, \tag{2}$$

with E_0 being the laser electric field peak amplitude. As we will see in the next section, by the integration of the Newton-Lorentz equation it is possible to obtain the time dynamics of the laser-ionized electron, as well as to estimate the classical electron kinetic energy as a function of the ionization and recombination times.

In order to complement the semiclassical analysis we compute the HHG spectra generated by the synthesized pulses of Fig. 3 by numerically integrating the 3D-TDSE in the length gauge within the dipole approximation. As it is well known, the harmonic yield of an atom is proportional to the Fourier transform of the dipole acceleration of its active electron. The latter can be calculated from the time-propagated electronic wave function. We have used our code which is based on an expansion in spherical harmonics, Y_l^m, considering only the $m = 0$ terms due to the cylindrical symmetry of the problem. The numerical technique to solve the 3D-TDSE is based on a Crank-Nicolson method implemented on a splitting of the time-evolution operator that preserves the norm of the wave function. Here, we focus our studies on the argon atom. This is so, considering this gas is one of the most commonly used in current HHG experiments. However, without loss of generality, the results explored in the present contribution can be extended to the rest of the noble gases. Hence, we have considered in our 3D-TDSE code the atomic potential reported in [31] to accurately describe the level structure of the argon atom under the SAE approximation. In addition, and in order to interpret the detailed spectral and temporal behavior of the HHG spectra, we perform a time-frequency analysis by means of a wavelet transform [32–34].

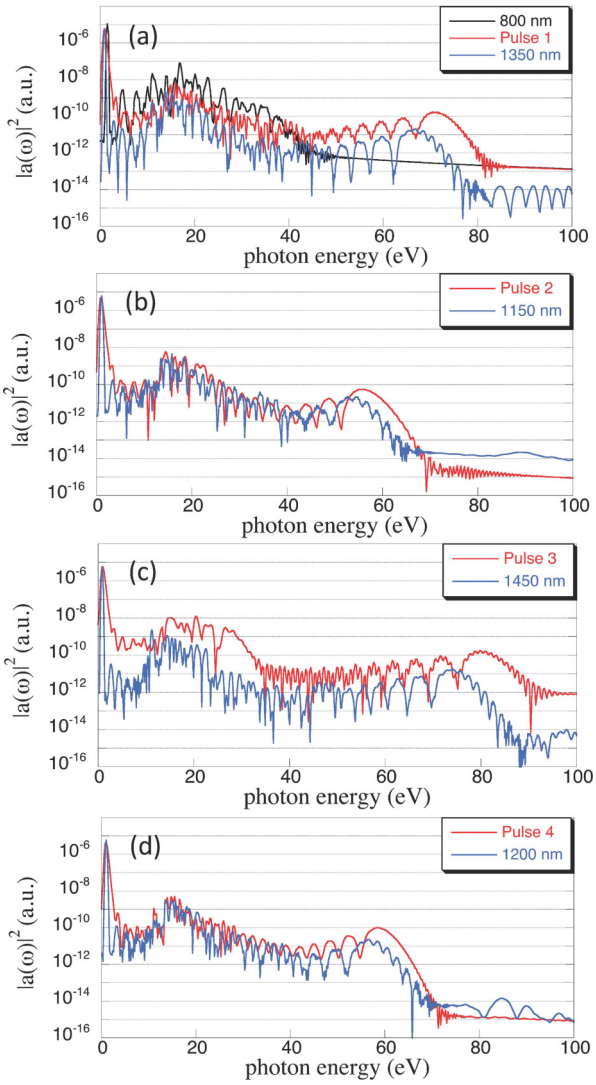

FIG. 4. 3D-TDSE HHG spectra in argon driven by the four synthesized pulses of Fig. 3 (red lines). (a) Pulse 1 [Fig. 3(a)]; (b) pulse 2 [Fig. 3(b)]; (c) pulse 3 [Fig. 3(c)]; and (d) pulse 4 [Fig. 3(d)]. In Fig. 4(a) the HHG spectrum (black line) for a conventional Gaussian pulse is included. Additionally, in all the panels the HHG spectra (blue lines) of their "equivalent pulses" are represented (see the text for details). The laser intensity is the same for all cases, $I = 10^{14}$ W/cm^2. The valley in the respective spectra around 40 eV is due to the Cooper minimum in argon [35].

III. RESULTS AND DISCUSSION

The initial pulse before the synthesis is a Gaussian pulse with one-cycle FWHM and a laser wavelength $\lambda_0 = 800$ nm [see Fig. 1(b)]. For the proposed pulse synthesis there is no particular laser intensity requirement, since a nonlinear medium is not necessary. Each of the four synthesized pulses

reach the argon atom ionization threshold at a laser electric field $E_0 = 0.053$ a.u. (see point A, Fig. 3). This value corresponds to a laser intensity $I = 10^{14}$ W/cm^2 and this is the value used in our simulations.

In Fig. 4 we show the HHG spectra that result from the interaction of argon atoms with the four synthesized pulses plotted in Fig. 3. In all cases we numerically integrated the 3D-TDSE under the SAE (red lines). The HHG spectra of Figs. 4(a)–4(d) correspond to the pulses of Figs. 3(a)–3(d), respectively. Additionally, in Fig. 4(a) we include the HHG spectrum corresponding to a laser wavelength $\lambda_0 = 800$ nm and intensity of 10^{14} W/cm^2 (black line). Finally, in Figs. 4(a)–4(d) the HHG spectra using "equivalent Gaussian pulses" (blue lines) are included (see below for details).

In each spectrum can be observed a noticeable increase of the cutoff, compared to the one obtained with a conventional Gaussian pulse with $\lambda_0 = 800$ nm and the same intensity. This result is expected since the synthesized pulses have approximately a wavelength of $\lambda \approx 1.5\lambda_0$ corresponding to $\lambda = 1200$ nm. However, pulses 1 and 3 have a cutoff extension that clearly exceeds the cutoff given by a pulse with a wavelength $\lambda = 1200$ nm. A possible explanation for the above phenomenon can be traced by considering the change in the electron trajectories in relation to those developed when a pure sine-like pulse is used. Our proposed synthesis generated chirped pulses, characterized for a certain degree of asymmetry in the temporal regions where the electron is ionized and recombines. This behavior was studied in previous works, where asymmetric pulses are obtained using different techniques [21,23–27].

Additionally, we analyze the HHG yield for each of the four proposed synthesized pulses. In order to interpret the asymmetry effects, we introduce a series of "equivalent Gaussian pulses" with a comparable wavelength, whose effect is to develop a similar HHG cutoff. The "equivalent pulse" is one constituted by a pure sine pulse, free of chirp, whose spectrum is peaked at the same central wavelength (center of gravity) as the synthesized pulse. Their associated HHG spectra are plotted in Figs. 4(a)–4(d) (blue lines). It can be observed that all synthesized pulses have larger HHG yields than the equivalent Gaussian ones. Pulses 1 and 3, the ones that produce larger cutoffs, show one order of magnitude increase in the harmonic yield compared to their equivalent pulse counterparts. Note that all spectra present a valley in the yield around 40 eV due to the argon Cooper minimum [35].

It is known that the HHG efficiency depends on the trajectory duration τ [14,17]. As a consequence, in order to explain the higher yield observed in the HHG spectra when the argon atoms are driven by the synthesized pulses, we study the travel times of the electrons in the continuum through a classical analysis. In Fig. 5 we show the classical total energies as a function of ionization (red points) and recombination (green

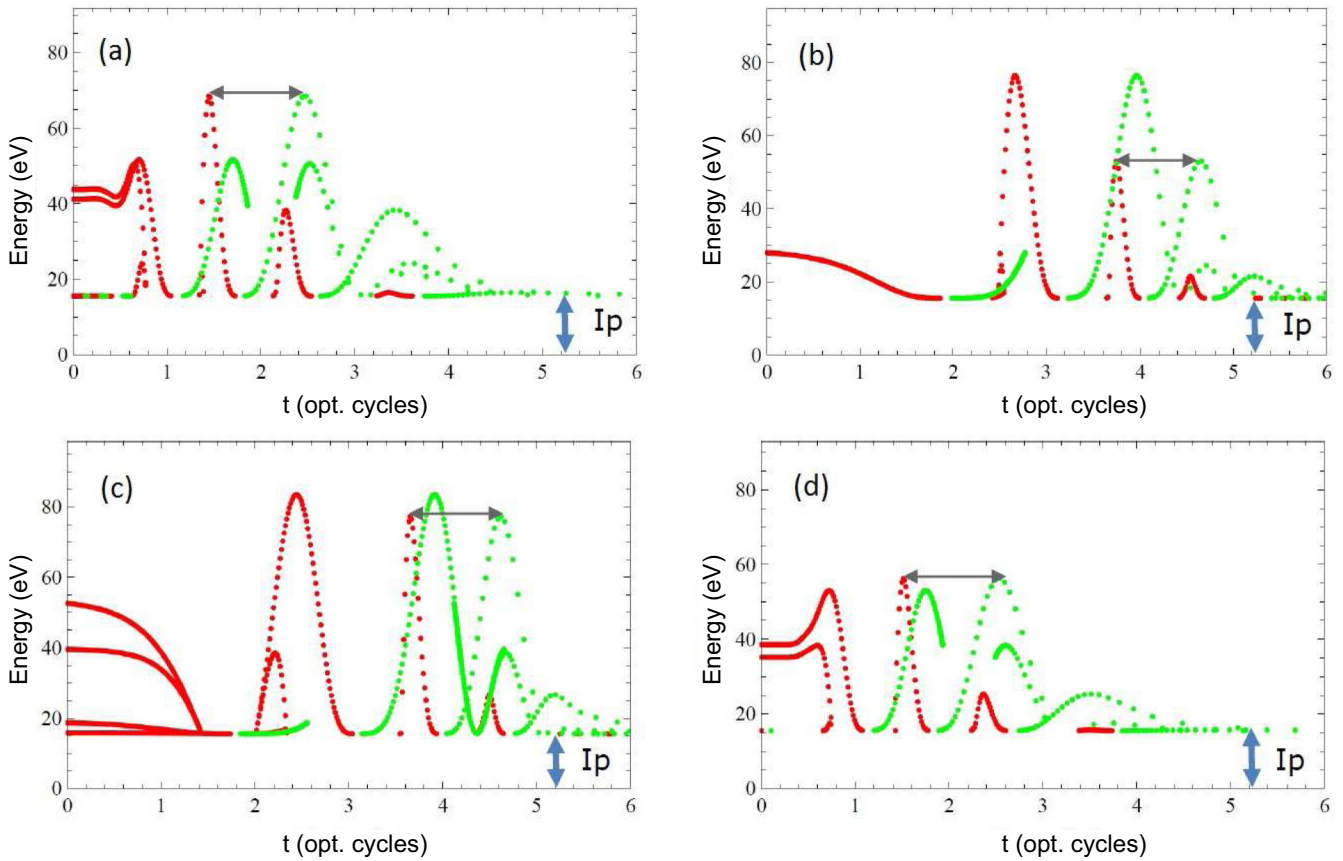

FIG. 5. Classical total electron energies (in eV) as a function of ionization (red points) and recombination (green points) times for the four synthesized pulses of Fig. 3. The black arrows show the travel times of the electron trajectories at the cutoff energy. The I_p (15.7 eV) of the argon atoms is displayed with blue arrows (note that one optical cycle is 2.66 fs).

TABLE I. Travel times τ for electrons at the cutoff energy for both synthesized and equivalent pulses.

	τ (fs) Synthesized	τ (fs) Equivalent
Pulse 1 ≡ 1350 nm	**2.70**	**3.29**
Pulse 2 ≡ 1150 nm	2.33	2.80
Pulse 3 ≡ 1450 nm	**2.38**	**3.53**
Pulse 4 ≡ 1200 nm	2.68	2.93

points) times (in optical cycles) for the four synthesized fields of Fig. 3. A quick inspection allows one to confirm the excellent correspondence between the classical cutoff energies and their quantum counterparts (see Fig. 4).

We perform a study comparing the travel times for the electron trajectories at the cutoff for both the synthesized and equivalent pulses. The former are extracted from the classical calculations (see the arrows in Fig. 5), meanwhile the latter are calculated as $\tau_G = 0.75T_p$ where $T_p = \frac{2\pi}{\omega}$ is the period of a pure sine wave with $\omega = \frac{2\pi c}{\lambda}$ (c is the speed of light). In Table I we present the numerical values of the travel times τ corresponding to the cases plotted in Fig. 5. The wavelengths indicated in the first column correspond to the spectral center of gravity of the synthesized pulses. We highlight in bold, the travel times of pulses 1 and 3, because in these cases longer cutoff energies and better efficiency are observed. It is shown that all travel times values for the synthesized pulses are smaller than those of the equivalent pulses. As a consequence, a higher HHG efficiency should be expected, considering that shorter travel times imply, in turn, less spread electron wave packets and thus larger recollision probabilities.

On the other hand, in order to confirm the previous results and clarify some aspects of the HHG process driven by these synthesized pulses, we perform a wavelet analysis of the HHG spectra of Fig. 4. We present the results in Fig. 6. From these plots we appreciate the temporal region in which the high-order harmonics are emitted. In Fig. 6(a) it is shown the wavelet analysis for black harmonic spectra [Fig. 4(a)] which correspond to the pure Gaussian pulse centered at 800 nm of wavelength. Figures 6(b) and 6(d) show three bursts of XUV radiation, meanwhile Figs. 6(c) and 6(e) present only two. As a consequence, the attosecond pulses associated with these burst will have different spectral and temporal characteristics. In addition, the classical electron energies at recombination are superimposed in the same plots (solid black lines). As observed, the classical results are in excellent agreement with the quantum mechanical ones.

As corollary we present the synthesis of attosecond pulses using the HHG spectra that have larger cutoff and higher efficiency, i.e. the ones corresponding to pulses 1 and 3 [Figs. 3(a) and 3(c)].

To obtain an IAP we use a 20 eV bandwidth filter close to the cutoff region, where only one event of electron recombination takes place. We show in Figs. 7(a) and 7(b) the HHG spectra jointly with a shadow region that represents the filter. In Figs. 7(c) and 7(d) we show the IAPs obtained. As shown, the IAP synthesized from pulse 3 is considerably shorter (260 as) than the IAP obtained from pulse 1 (490 as).

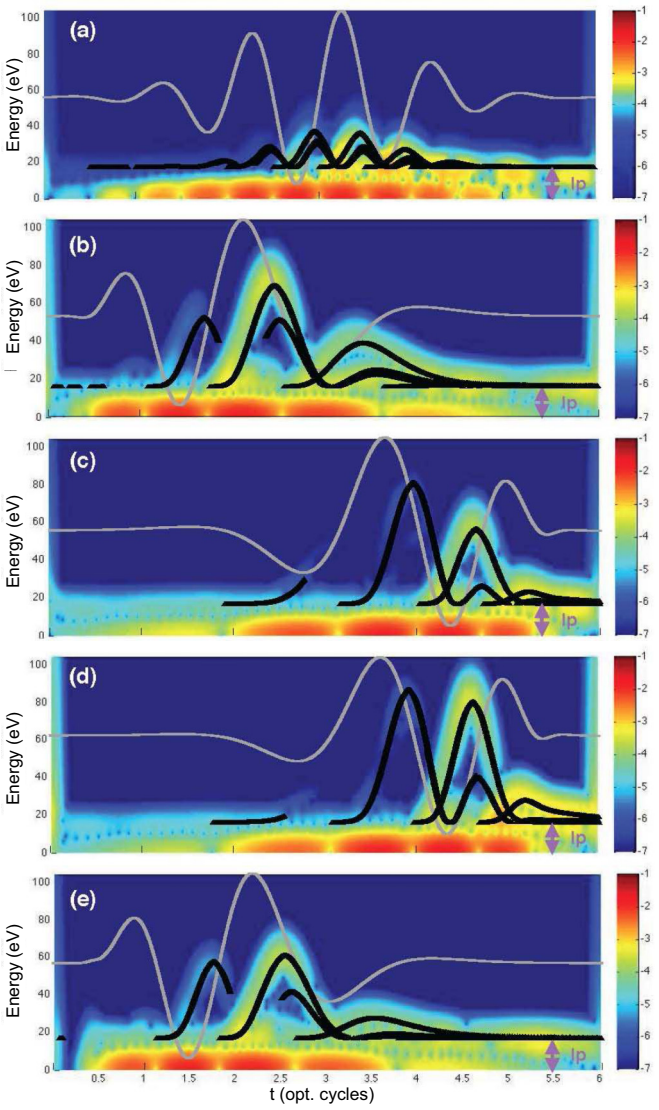

FIG. 6. Time-frequency analysis of the HHG spectra of Fig. 4. The classical electron energies at the recombination time is superimposed (solid black lines). The driving pulses are also plotted (solid gray line). The laser intensity is the same for all cases, $I = 10^{14}$ W/cm^2.

IV. CONCLUSIONS AND OUTLOOK

We have proposed an experimental approach to synthesizing an approximately one-cycle laser pulse with a wavelength of $\lambda \approx 1.5\lambda_0$, from an input pulse with wavelength of λ_0. We analyze four synthesized pulses with different characteristics and certain degrees of chirp, all of them being obtained by varying the lengths L_1 and L_2 of a dispersive material, as well as the sign of its GVD.

We study the HHG process in argon atoms driven by those pulses, both by solving the Schrödinger equation in full dimensionality (3D-TDSE) and the classical analysis. All synthesized pulses give rise to an extension of the cutoff energy and a larger efficiency of the harmonic yield.

To compare the efficiency of the harmonics yield we introduce four equivalent pulses that produce the same cutoffs as the four synthesized pulses. We show that the HHG yields using the

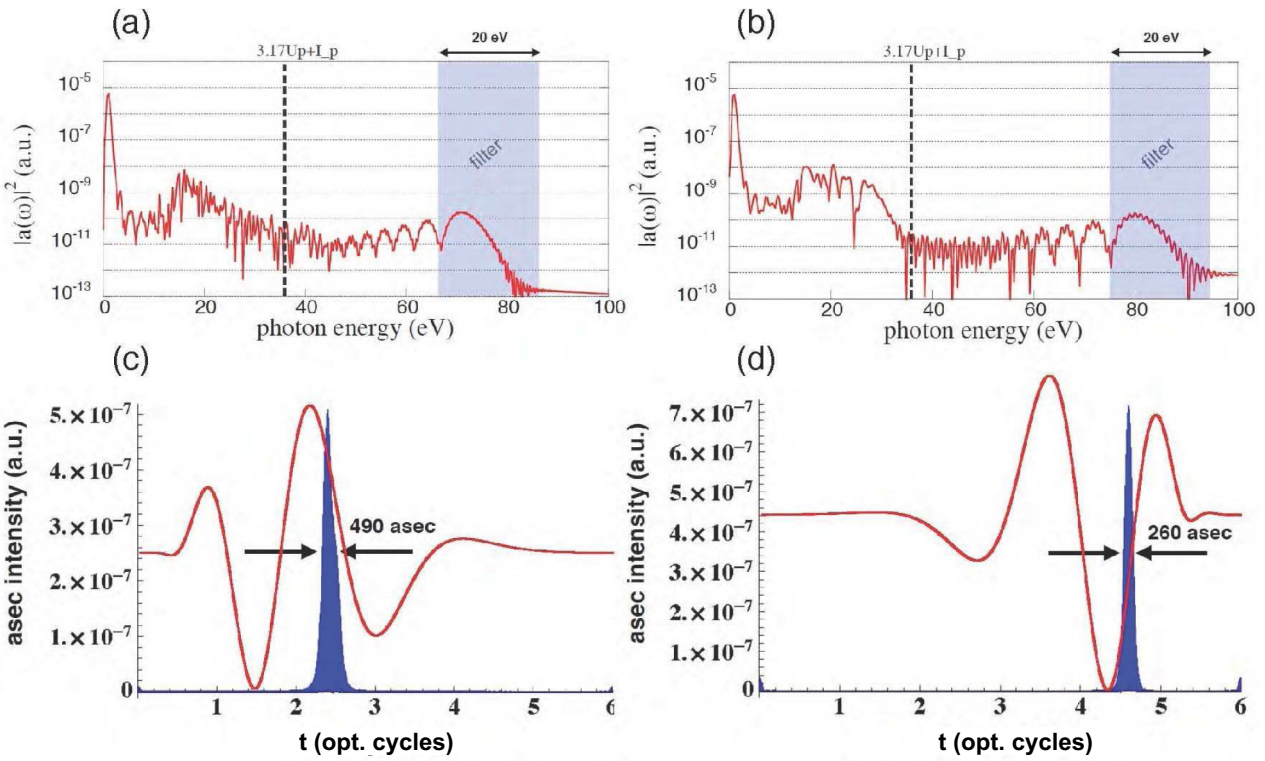

FIG. 7. HHG generated by (a) pulse 1 and (b) pulse 3 and the corresponding attosecond pulses (c) and (d), respectively, using a 20 eV filter in the cutoff region.

synthesized pulses have an efficiency one order of magnitude larger than their equivalent counterparts. By carefully studying the travel times of electrons in the continuum through the classical analysis of the ionization-recombination energies we are able to explain the reasons for this behavior in the HHG spectra.

In summary, we show a possible experimental setup to synthesize an approximately one-cycle optical pulse to enhance both the HHG cutoff and yield. These improvements can be understood considering that the synthesized pulses have a certain degree of asymmetry in the ionization-recombination temporal region. This introduces noticeable changes in the electron trajectories when compared with a pure sine pulse. Likewise this technique can be used to generate attosecond pulses with multicycle driven pulses.

ACKNOWLEDGMENTS

This work was partially supported by the Agencia Nacional de Promoción Científica y Tecnológica (Argentina) under Project PICT-2016-4086. The results of the Project LQ1606 were obtained with the financial support of the Ministry of Education, Youth and Sports as part of targeted support from the National Programme of Sustainability II. Supported by the project Advanced research using high intensity laser produced photons and particles (CZ.02.1.01/0.0/0.0/16_019/0000789) from European Regional Development Fund (ADONIS). J.A.P.H. and L.R. acknowledge Spanish Ministerio de Economía, Industria y Competitividad (MINECO) through the PALMA Grant No. FIS2016-81056-R, from LaserLab Europe IV Grant No. 654148, and from the Regional Government, Junta de Castilla y León, Grant No. CLP087U16.

[1] B. E. Schmidt, P. Béjot, M. Giguère, A. D. Shiner, C. Trallero-Herrero, É. Bisson, J. Kasparian, J.-P. Wolf, D. M. Villeneuve, J.-C. Kieffer *et al.*, Compression of 1.8 μm laser pulses to sub two optical cycles with bulk material, Appl. Phys. Lett. **96**, 121109 (2010).

[2] S. Driever, D. Bigourd, N. Fedorov, M. Cornet, M. Arnold, F. Burgy, S. Montant, S. Petit, D. Descamps, E. Cormier, E. Constant, and A. Zaïr, Tunable 1.6–2 μm near infrared few-cycle pulse generation by filamentation, Appl. Phys. Lett. **102**, 191119 (2013).

[3] D. Brida, C. Manzoni, G. Cirmi, M. Marangoni, S. Bonora, P. Villoresi, S. De Silvestri, and G. Cerullo, Few-optical-cycle pulses tunable from the visible to the mid-infrared by optical parametric amplifiers, J. of Opt. **12**, 013001 (2009).

[4] S.-W. Huang, G. Cirmi, J. Moses, K.-H. Hong, S. Bhardwaj, J. R. Birge, L.-J. Chen, E. Li, B. J. Eggleton, G. Cerullo, and F. X Kärtner, High-energy pulse synthesis with sub-cycle waveform control for strong-field physics, Nat. Photon. **5**, 475 (2011).

[5] J. A. Cox, W. P. Putnam, A. Sell, A. Leitenstorfer, and F. X. Kärtner, Pulse synthesis in the single-cycle regime from independent mode-locked lasers using attosecond-precision feedback, Opt. Lett. **37**, 3579 (2012).

[6] C. Manzoni, O. D. Mücke, G. Cirmi, S. Fang, J. Moses, S.-W. Huang, K.-H. Hong, G. Cerullo, and F. X. Kärtner, Coherent

pulse synthesis: towards sub-cycle optical waveforms, Laser Photon. Rev. **9**, 129 (2015).

[7] G. Sansone, E. Benedetti, F. Calegari, C. Vozzi, L. Avaldi, R. Flammini, L. Poletto, P. Villoresi, C. Altucci, R. Velotta, S. Stagira, S. De Silvestri, and M. Nisoli, Isolated single-cycle attosecond pulses, Science **314**, 443 (2006).

[8] C. Krausz and M. I. Stockman, Attosecond metrology: from electron capture to future signal processing, Nat. Photon. **8**, 205 (2014).

[9] C. Altucci, R. Esposito, V. Tosa, and R. Velotta, Single isolated attosecond pulse from multicycle lasers, Opt. Lett. **33**, 2943 (2008).

[10] C. Altucci, R. Velotta, V. Tosa, P. Villoresi, F. Frasseto, L. Poletto, C. Vozzi, F. Calegari, M. Negro, S. De Silvestri, and S. Stagira, Interplay between group-delay-dispersion-induced polarization gating and ionization to generate isolated attosecond pulses from multicycle lasers, Opt. Lett. **35**, 2798 (2010).

[11] J. L. Krause, K. J. Schafer, and K. C. Kulander, High-Order Harmonic Generation from Atoms and Ions in the High Intensity Regime, Phys. Rev. Lett. **68**, 3535 (1992).

[12] A. L'Huillier and Ph. Balcou, High-Order Harmonic Generation in Rare Gases with a 1-ps 1053-nm Laser, Phys. Rev. Lett. **70**, 774 (1993).

[13] J. J. Macklin, J. D. Kmetec, and C. L. Gordon III, High-Order Harmonic Generation using Intense Femtosecond Pulses, Phys. Rev. Lett. **70**, 766 (1993).

[14] J. Tate, T. Auguste, H. G. Muller, P. Saliéres, P. Agostini, and L. F. DiMauro, Scaling of Wave-Packet Dynamics in an Intense Midinfrared Field, Phys. Rev. Lett. **98**, 013901 (2007).

[15] J. A. Pérez-Hernández, L. Roso, and L. Plaja, Harmonic generation beyond the strong-field approximation: the physics behind the short-wave-infrared scaling laws, Opt. Exp. **17**, 9891 (2009).

[16] M. V. Frolov, N. L. Manakov, and A. F. Starace, Wavelength Scaling of High-Harmonic Yield: Threshold Phenomena and Bound State Symmetry Dependence, Phys. Rev. Lett. **100**, 173001 (2008).

[17] P. Colosimo, G. Doumy, C. I. Blaga, J. Wheeler, C. Hauri, F. Catoire, J. Tate, R. Chirla, A. M. March, G. G. Paulus, H. G. Muller, P. Agostini, and L. F. DiMauro, Scaling strong-field interactions towards the classical limit, Nat. Phys. **4**, 386 (2008).

[18] V. V. Strelkov, A. F. Sterjantov, N. Yu. Shubin, and V. T. Platonenko, XUV generation with several-cycle laser pulse in barrier-suppression regime, J. Phys. B **39**, 577 (2006).

[19] P. Moreno, L. Plaja, V. Malyshev, and L. Roso, Influence of barrier suppression in high-order harmonic generation, Phys. Rev. A **51**, 4746 (1995).

[20] J. A. Pérez-Hernández, R. Guichard, A. Zaïr, L. Roso, and L. Plaja, Valley structure in the harmonic efficiency at ultra-high laser intensities, in *High Intensity Lasers and High Field Phenomena* (Optical Society, Washington, 2012), p. HT4C–8.

[21] J. A. Pérez-Hernández, D. J. Hoffmann, A. Zaïr, L. E. Chipperfield, L. Plaja, C. Ruiz, J. P. Marangos, and L. Roso, Extension of the cut-off in high-harmonic generation using two delayed pulses of the same colour, J. Phys. B **42**, 134004 (2009).

[22] J. A. Pérez-Hernández, M. F. Ciappina, M. Lewenstein, L. Roso, and A. Zaïr, Beyond Carbon k-Edge Harmonic Emission using a Spatial and Temporal Synthesized Laser Field, Phys. Rev. Lett. **110**, 053001 (2013).

[23] L. E. Chipperfield, J. S. Robinson, J. W. G. Tisch, and J. P. Marangos, Ideal Waveform to Generate the Maximum Possible Electron Recollision Energy for any Given Oscillation Period, Phys. Rev. Lett. **102**, 063003 (2009).

[24] P. Wei, J. Miao, Z. Zeng, C. Li, X. Ge, R. Li, and Z. Xu, Selective Enhancement of a Single Harmonic Emission in a Driving Laser Field with Subcycle Waveform Control, Phys. Rev. Lett. **110**, 233903 (2013).

[25] I. J. Kim, C. M. Kim, H. T. Kim, G. H. Lee, Y. S. Lee, J. Y. Park, D. J. Cho, and C. H. Nam, Highly Efficient High-Harmonic Generation in an Orthogonally Polarized Two-Color Laser Field, Phys. Rev. Lett. **94**, 243901 (2005).

[26] E. Neyra, F. Videla, J. A. Pérez-Hernández, M. F. Ciappina, L. Roso, and G. A. Torchia, High-order harmonic generation driven by chirped laser pulses induced by linear and non linear phenomena, Eur. Phys. J. D **70**, 243 (2016).

[27] E. Neyra, F. Videla, J. A. Pérez-Hernández, M. F. Ciappina, L. Roso, and G. A. Torchia, Extending the high-order harmonic generation cutoff by means of self-phase-modulated chirped pulses, Laser Phys. Lett. **13**, 115303 (2016).

[28] M. Lara-Astiaso, R. E. F. Silva, A. Gubaydullin, P. Rivière, C. Meier, and F Martín, Enhancing High-Order Harmonic Generation in Light Molecules by using Chirped Pulses, Phys. Rev. Lett. **117**, 093003 (2016).

[29] P. B. Corkum, Plasma Perspective on Strong Field Multiphoton Ionization, Phys. Rev. Lett. **71**, 1994 (1993).

[30] M. Lewenstein, Ph. Balcou, M. Yu. Ivanov, A. L'Huillier, and P. B. Corkum, Theory of high-harmonic generation by low-frequency laser fields, Phys. Rev. A **49**, 2117 (1994).

[31] X.-M. Tong and C. D. Lin, Empirical formula for static field ionization rates of atoms and molecules by lasers in the barrier-suppression regime, J. Phys. B **38**, 2593 (2005).

[32] C. K. Chui, *An Introduction to Wavelets* (Elsevier, New York, 2016).

[33] Ph. Antoine, B. Piraux, and A. Maquet, Time profile of harmonics generated by a single atom in a strong electromagnetic field, Phys. Rev. A **51**, R1750 (1995).

[34] X.-M. Tong and S.-I. Chu, Probing the spectral and temporal structures of high-order harmonic generation in intense laser pulses, Phys. Rev. A **61**, 021802(R) (2000).

[35] J. W. Cooper, Photoionization from outer atomic subshells. A model study, Phys. Rev. **128**, 681 (1962).